



OPEN

Induced changes of pyrolysis temperature on the physicochemical traits of sewage sludge and on the potential ecological risks

Claudineia de Souza Souza, Marcela Rebouças Bomfim[✉], Maria da Conceição de Almeida, Lucas de Souza Alves, Welder Neves de Santana, Itamar Carlos da Silva Amorim & Jorge Antonio Gonzaga Santos

Biochar from sewage sludge is a low-cost sorbent that may be used for several environmental functions. This study evaluates the induced effects of pyrolysis temperature on the physicochemical characteristics of sewage sludge (SS) biochar produced at 350 (SSB₃₅₀), 450 (SSB₄₅₀) and 600 (SSB₆₀₀), based on the metal enrichment index, metal mobility index (MMI), and potential ecological risk index (PERI) of Cd, Cu, Pb, and Zn. Increased pyrolysis temperature reduced the biochar concentration of elements that are lost as volatile compounds (C, N, H, O, and S), while the concentration of stable aromatic carbon, ash, alkalinity, some macro (Ca, Mg, P₂O₅, and K₂O) and micronutrients (Cu and Zn), and toxic elements such as Pb and Cd increased. Increasing the pyrolysis temperature is also important in the transformation of metals from toxic and available forms into more stable potentially available and non-available forms. Based on the individual potential ecological risk index, Cd in the SS and SSB₄₅₀ were in the moderate and considerable contamination ranges, respectively. For all pyrolysis temperature biochar Cd was the highest metal contributor to the PERI. Despite this, the potential ecological risk index of the SS and SSBs was graded as low.

Biochar is a stabilized, recalcitrant organic carbon compound produced by pyrolysis¹ when biomass is heated under low oxygen concentrations² to temperatures usually between 300 and 1000 °C. The feedstock source, characteristics of the pyrolysis process largely determine the suitability of biochar for a given application³. Biochar physical (specific surface area, pore size and distribution); chemical (presence of functional groups, such as carboxyl, hydroxyl, phenolic, and aromatics⁴, and nutritional (phosphorus, nitrogen, sulphur, and micronutrients) characteristics⁵ are largely controlled by the raw material source and pyrolysis process. The diversity of physicochemical characteristics of biochar has allowed the tailoring of the material for use as an agricultural amendment⁶, for sequestration of carbon, and as a sorbent for potentially hazardous organic and inorganic compounds in aquatic environment, soil, and sediments⁷. It also has applications in mitigation of climate change⁸, energy production^{3,9} industry, and engineering¹⁰. One of the reasons for the wide acceptance of biochar use is the possibility of reuse of different biomass sources, such as garbage or refuse, sludge from waste treatment plants, and discarded material resulting from industrial, commercial, mining, agricultural, and community activities¹¹.

The disposal of sewage sludge (SS) in landfills and by incineration has been gradually replaced by the use of the material for biochar production. Use of traditional disposal methods has reduced due to land limitations, secondary contaminant production, and the risk of polluting farmland and surface or subsurface water. Solid SS from wastewater treatment has received attention as a biomass source for biochar production^{12,13}, and is used in agriculture because of its high nitrogen, phosphorus, and micronutrient content. One of the advantages of using SS from waste water treatment plants (WWTPs) as a sustainable source for biochar production is its worldwide

Universidade Federal Do Recôncavo da Bahia, Rua Rui Barbosa, 710, Cruz das Almas, BA, Brazil. ✉email: reboucas.marcela@gmail.com

availability, and the tendency for its production to increase over time due to an increase in global population and the number of households connected to SS systems in developing countries.

The use of SS for biochar production mitigates the problems caused by SS waste volume; presence of harmful pharmaceuticals; pathogenic vectors and organisms; and potentially toxic elements (PTEs), and reduces the amount of carbon released to the atmosphere¹². The resultant biochar is a pathogen-free material with great potential for immobilizing inorganic contaminants¹³, and PTEs are transformed into less toxic forms¹⁴.

Pyrolysis has been developed as a sustainable treatment technique for sludge management because it has the potential to simultaneously target energy recovery, nutrient recycling, heavy metal immobilization, and environmental protection¹⁵. The heating rate, residence time, and temperature have a direct impact on biochar characteristics¹⁶. Biochar produced at high temperatures has a high carbon content, large surface area, and low reactivity functional groups, as indicated by the low H/C and O/C molar ratios, reflecting the loss of highly degradable compounds through dehydration and decarboxylation reactions¹⁷.

Although biochar production and use offer many opportunities for enhancing soil and environmental health quality, for use on a large scale, individual and environmental safety protocols must be adopted to regulate feedstock quality, pyrolysis processes, and certification of the final product to indicate its suitability for further use.

Garbage or refuse, sludge from waste treatment plants, and material discarded during industrial, commercial, mining, agricultural, and community activities may contain toxic levels of PTEs¹⁸, polycyclic aromatic hydrocarbons (PAH), polychlorinated dibenzodioxins (PCDDs), polychlorinated dibenzofurans (PCDFs) polychlorinated biphenyl (PCB), inorganic pesticides, dioxins, persistent organic pollutants (POPs)^{19,20}, toxins²¹; glass, hard plastic, film plastic, metals, textiles²²; and polyvinyl chloride (PVC)²³. Protection against cytotoxicity caused by fine biochar particles commonly released during biochar production and field application²⁴ is a further health risk that needs to be assessed.

The total PTE concentration in the biochar matrix is a useful pollution indicator of content but it provides no information on the metals environment impact, which depends on their chemical form²⁵. The data produced by the chemical speciation or sequential extraction allows to determine the mobile, bioavailable PTEs forms in the sludge and biochar²⁶ which may limit the disposal and utilization due to their environmental risk.

The potential ecological risk index (PERI) proposed by Ref.²⁷ may be used as an important tool to evaluate the detrimental effect of PTEs present in the biochar biomass to the microbial populations on plants, animals, and humans²⁸. The PERI index integrates a single-element potential ecological risk (Er) for all PTEs present in a sample¹⁸. Despite the need to evaluate other ecotoxicological factors that may restrict the use of biochar in the environment, this study was undertaken with the specific objectives of evaluating the effect of pyrolysis temperature on SS biochar: (1) physicochemical characteristics, (2) availability of PTE, defined here as Cd, Cu, Pb, and Zn, and (3) the potential ecological risk as a means of providing a scientific basis for the safe and eco-friendly use of the material.

Materials and methods

Biochar production. The SS used in this study was derived from the WWTP of the Bahian Water and Sanitation Company (EMBASA) in Cruz das Almas, Bahia State, Brazil. The feedstock was air-dried and then pyrolyzed at temperatures of 350, 450 and 600 °C, and the resultant biochar is hereafter referred to as SSB₃₅₀, SSB₄₅₀, and SSB₆₀₀, respectively. The pyrolysis process of the sludge was carried out by a third-party company (Bahiacarbon Agroindustrial LTDA) at a rate of 10 °C min⁻¹ until the target temperature was reached, with an average yield of 5–10%. The final temperature was maintained for 2 h; the sample was then cooled slowly to room temperature. The SSB was homogenized and screened to pass through a 2 mm stainless sieve.

Ultimate and proximate analysis. The ultimate analyses (C, H, N, and S concentrations) of the sewage sludge (SS) and sewage sludge biochar (SSB) were determined using an automatic elemental analyzer (Vario EL III, Elementar, Hanau, Germany). The percentage of oxygen in the samples was calculated according to the formula 1:

$$\text{O}(\%) = 100 - (\text{C} \% + \text{H} \% + \text{N} \% + \text{S} \% + \text{ash} \%) \quad (1)$$

The proximate analysis [moisture, ash, volatiles, and fixed carbon (FC)] of the sewage sludge (SS) and sewage sludge biochar (SSB) were determined using different procedures. The moisture content was determined by the weight loss of the sample as it was heated to 150 °C. The volatile content was determined as the sample was heated from 150 to 750 °C in a muffle (Linn-Elektro Therm model N 480 D). The ash content of each sample was measured by dry combustion in a muffle furnace at 750 °C for 6 h²⁹. Fixed carbon was calculated according to the formula 2:

$$\text{FC}(\%) = 100\% - (\text{moisture} \% - \text{volatile matter} \% - \text{ash} \%) \quad (2)$$

Characteristics of the mineral fractions. The total metal concentration in the biochar was determined in 5 cm of macerated and homogenized samples deposited in 20 cm acrylic capsules. sealed with a 0.2 mm thick polypropylene film. The samples were analyzed by the method 6200³⁰ using energy dispersive portable X-ray fluorescence (PXRF) spectrometry (Brucker, model Titan 600).

The metal concentration was also determined in a 3050B extract³¹ by atomic absorption spectroscopy (Varian, model FS 240F). Samples of 0.5 g of SS and SSB were digested in 5 mL of 2 M HNO₃ solution together with 2 mL H₂O₂ (30%) and the volume was made up to 50 mL with Milli-Q water.

Physicochemical characteristics. The feedstock and SSB samples were suspended in deionized water and 1 M KCl (1:10 m/v ratio), stirred for 30 min and allowed to stand for 5 min, then assessed for $\text{pH}_{(\text{H}_2\text{O})}$ and $\text{pH}_{(\text{KCl})}$, respectively, using a pH meter (Hanna, model HI 3221). The electroconductivity (EC) was analyzed using a conductivity meter (Tecnal, model 4 MP).

Cation exchange capacity (CEC) was measured as described by Ref.³². In summary, 25 g of each biochar sample and 125 mL of 1 M NH_4OAc were transferred into 200 mL vessels and shaken on a reciprocal shaker for 15 h. The vessel contents were poured through a filter paper-fitted Buchner funnel. Each flask containing biochar was rinsed four times with 25 mL NH_4OAc to remove biochar stuck onto container sides and the leachate was discarded. The biochar on the filter paper was rinsed eight times by adding 25 mL of 95% $\text{CH}_3\text{CH}_2\text{OH}$ to remove the excess NH_4^+ adsorbed. The NH_4^+ adsorbed in the biochar was displaced with 1 M KCl. The leachate was transferred to a 250 mL volumetric flask and the volume was made up to 250 mL with 1 M KCl. The concentration of NH_4^+ in the KCl extract was determined by Spectro colorimetry analysis (PerkinElmer Model Lambda 25 UV/Vis) at $\lambda = 400$ nm. The concentration of NH_4^+ was determined in both the sample and the blank KCl extraction solution. The concentration of NH_4^+ was calculated using the Nessler method³³ according to Eq. (3):

$$\text{CEC} = \frac{\text{NH}_4^+ \text{ Extractant} - \text{NH}_4^+ \text{ Blank}}{14} \quad (3)$$

where CEC is the cation exchange capacity ($\text{cmol}_c \text{ kg}^{-1}$); NH_4^+ Extractant is the concentration of NH_4^+ adsorbed by the biochar (mg L^{-1}) and NH_4^+ Blank is the concentration of NH_4^+ in the blank extractant solution (mg L^{-1}).

Speciation of potential toxic metals (PTEs). The chemical speciation of PTEs (Cu, Cd, Pb, and Zn) in the SS and SSBs were carried out according to Tessier et al.³⁴ tests. The water-soluble fraction (F1) was extracted with Milli-Q water for 18 h; the exchangeable fraction (F2) was extracted with 1 M MgCl_2 at pH 7 for 1 h; the carbonate fraction (F3) was extracted with 1 M CH_3COONa at pH 5 for 5 h; the weakly crystalline Fe and Mn oxides fraction (F4) was extracted with 0.04 M NH_2OH in 25% (V/V) CH_3COOH (pH 2) for 6 h at 96 °C; the organic matter fraction F5 was extracted for 2 h at 85 °C with 3 mL of 0.02 M HNO_3 and 5 mL of 30% H_2O_2 adjusted to pH 2 with HNO_3 , with occasional agitation; the residual fraction (F6) was extracted with 20 mL of 7 M HNO_3 for 6 h at 80 °C. After each extraction, a washing step was performed to collect the remaining extractant solution. The solutions from the extraction and washing steps were combined for chemical analysis. After each extraction procedure, the mixture was centrifuged (Hettich 420R) at 3000 rpm for 30 min, and the supernatant was collected and filtered (<0.45 mm). The metal content of each fraction was determined by atomic absorption spectroscopy (Varian FS 240F).

Potential toxic metals and mobility enrichment index (MEI). The metal enrichment index (MEI), ratio of the PTE concentration in the biochar sample (SSB), and the background metal concentration (for SS) were used to evaluate the influences of pyrolysis temperatures on SSB metal enrichment. The MEI was calculated using Eq. (4):

$$\text{MEI} = \frac{C_i \text{ biochar}}{C_i \text{ SS}} \quad (4)$$

where C_i biochar and C_i SS are the PTE concentrations where i (i.e., Pb, Cu, Cd, and Zn) is determined for the biochar produced at a given pyrolysis temperature, and in the SS, respectively. The metal mobility index (MMI) of the PTEs in the SS and SSBs measuring the metal availability and mobility in SS and biochar was calculated according to Kabala and Singh³⁵, Eq. (5). The most labile fraction (F1, F2, and F3) of each metal was divided by the total metal concentration (F1 + F2 + F3 + F4 + F5 + F6).

$$\text{MMI} = \frac{F1 + F2 + F3}{F1 + F2 + F3 + F4 + F5 + F6} \times 100 \quad (5)$$

Potential ecological risk index (PERI). The potential ecological risk index (PERI) proposed by Hakanson²⁷ was used to evaluate the potential ecological risk of PTEs in biochar produced at different temperatures. The method takes into consideration the toxic level, total concentration, and ecological sensitivity to PTEs³⁶. The PERI was calculated according to the steps described by Eqs. (6, 7 and 8):

$$C_f = \frac{C_m}{C_n} \quad (6)$$

$$ER = Tr * C_f \quad (7)$$

$$RI = \sum Er \quad (8)$$

where C_f is the contamination factor, a measure of the degree of pollution on PTE; C_m and C_n are the concentrations of each PTE in the mobile (F1 + F2 + F3) and stable fractions (F4 + F5 + F6) respectively; T_r is the biological toxic factor for individual metals: Zn (1), Cu (5), Pb (5), and Cd (30)²⁷; E_r is the potential ecological risk index of a single element; PERI is the potential ecological risk index of the overall contamination. The values of C_f , E_r , and PERI were used to assess the risk of metal in the SS and the different pyrolysis temperature SSBs.

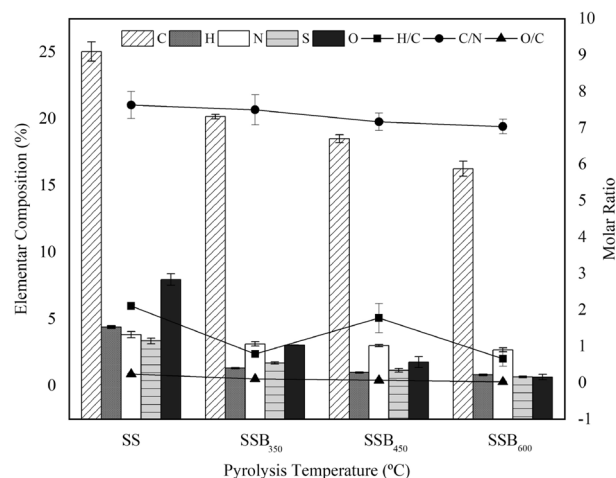


Figure 1. Ultimate analysis of sewage sludge (SS) and sewage sludge biochar (SSB) produced at the pyrolysis temperatures of 350 (SSB₃₅₀), 450 (SSB₄₅₀) and 600 (SSB₆₀₀).

Experimental design. The study was carried out as a completely randomized design with four treatments (SS, SSB₃₅₀, SSB₄₅₀, and SSB₆₀₀), and four repetitions. One-way analysis of variance (ANOVA) was performed for all variables. For variables that present significant effects ($p < 0.05$), the means were separated using the least significant difference (LSD) test at $p < 0.05$. The computer-based software SPSS V25³⁷ was used for descriptive statistical analyses. When necessary, the software was used to adjust the linear regression.

Results and discussion

Ultimate and proximate analysis. When compared to biochar produced from other feedstocks, sewage biochar is characterized by low C, N, and H values, especially C^{38,39}. In this study, the C ($C (\%) = -0.01 \text{ PYTemp} + 25.10$, $R^2 = 0.98$), N ($\%N = -0.002 \text{ PYTemp} + 3.832$, $R^2 = 0.89$), H ($H (\%) = -0.01 \text{ PYTemp} + 4.14$, $R^2 = 0.92$), O ($O (\%) = -0.01 \text{ PYTemp} + 7.76$, $R^2 = 0.98$), and S ($S (\%) = -0.01 \text{ PYTemp} + 3.342$, $R^2 = 0.98$) contents decreased with increasing pyrolysis temperature (PYTemp) (Fig. 1). The elementary content of C ($25.04 \pm 0.72\%$), N ($3.84 \pm 0.23\%$), H ($4.41 \pm 0.09\%$), S ($3.37 \pm 0.21\%$) and O ($7.96 \pm 0.43\%$) in the SS was higher than C ($16.26 \pm 0.56\%$), N ($2.70 \pm 0.15\%$), H ($0.83 \pm 0.03\%$), S ($0.67 \pm 0.06\%$), and O ($0.66 \pm 0.20\%$) of the SSB₆₀₀.

The reduction of C and O in the biochar occurs mostly by the volatilization of the elements as CO, CO₂, H₂O, and hydrocarbon during pyrolysis⁴⁰. Additional loss of O alone or associated with H occurs during pyrolysis due to the reduction of the hydroxyl (-OH) functional groups, dehydration, and condensation processes⁴¹. Decreases in the H content with increasing pyrolysis temperature have also been reported for other feedstocks^{5,12}. Nitrogen is lost mainly by the volatilization of different nitrogen groups such as NH₄-N or NO₃-N at low temperatures⁴², and pyridine at temperatures > 600 °C⁴³. The decrease in S with temperature has been reported in other studies^{44,45}. The loss of S from the biochar is due to sulfur containing volatile organic compounds. Organic sulfur losses to the vapor phase during pyrolysis have been primarily identified as carbonyl sulfide⁴⁶.

The reflex of the pyrolysis temperature on the reduction of C, H, N, O, and S is the change in key biochar treatments such as the H/C molar ratio, an index of the biochar aromaticity and stability; the O/C molar ratio, an index of polarity or the abundance of polar oxygen-containing surface functional groups⁴⁷; and the C/N molar ratio, an index of inorganic N release from organic matter when biochar is incorporated into soils⁴⁸.

The H/C and O/C molar ratios reduced with pyrolysis temperature and ranged from 2.11 ± 0.04 (SS) to 0.61 ± 0.02 (SSB₆₀₀), and from 0.24 ± 0.02 (SS) to 0.03 ± 0.01 (SSB₆₀₀). Plotting the H/C and O/C molar ratios in a van Krevelen diagram (Fig. 2) shows the reduction of the molar ratio with the increase of pyrolysis temperature. This result is in agreement with the results reported by Zhang et al.⁴⁹, where evaluation of biochar from cow manure produced at 300, 400, 500, 600, and 700 °C also reported H/C and O/C molar reduction with increase of temperature and attributed the results to the formation of stable aromatic structures. According to Ahmad et al.⁹, at pyrolysis temperatures up to 480 °C, the decrease in H/C and O/C molar ratio with increasing temperature is due to the loss of carboxylic and phenolic functional groups that are responsible for the CEC; above 480 °C, the reduction occurs due to the processes of dehydration and deoxygenation, which reduce H- and O-containing functional groups.

The C/N molar ratio of the SS (7.63 ± 0.37) did not differ from those of SSB₃₅₀ (7.50 ± 0.37) and SSB₄₅₀ (7.17 ± 0.24), but it was reduced in the SSB₆₀₀ (7.04 ± 0.20) as a result of the formation of compounds rich in C and poor in volatile N^{50,51}. According to Jindo et al.⁵², the biochar from lignocellulosic material ranged from 40 to 256; thus, the low C/N ratio of the biochar in this study revealed the SSB potential as a source of N for plants.

Proximate analysis typically involves the determination of volatile matter, moisture, fixed carbon (FC), and ash⁵³. Pyrolysis reduced the volatile content by up to 83% (from SS 36.6 ± 0.7 to SSB₆₀₀ 6.3 ± 0.3) due to the transformation of compounds containing O=C=O into gas⁵³, leading to an increase in the concentration of Si, Al, and Fe oxides with increasing temperature. Working with sewage sludge pyrolyzed at temperatures from 300

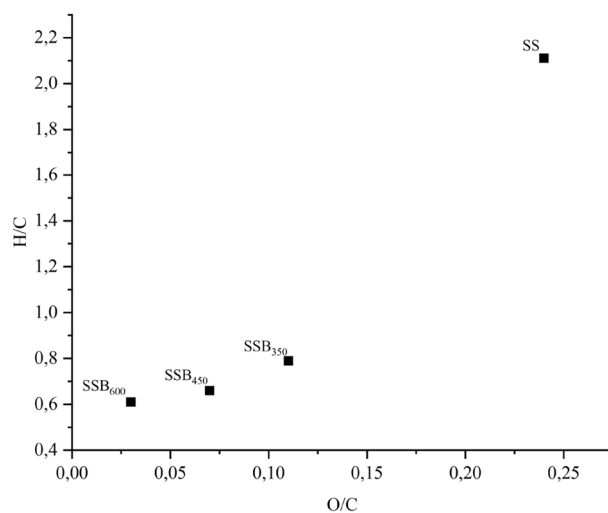


Figure 2. van Krevelen diagram for sewage sludge (SS) and sewage sludge biochar (SSB) produced at the pyrolysis temperatures of 350 (SSB₃₅₀), 450 (SSB₄₅₀) and 600 (SSB₆₀₀).

Biochar characteristic	SS	SSB ₃₅₀ ^a	SSB ₄₅₀ ^a	SSB ₆₀₀ ^a
Moisture (%)	7.3 ± 0.0	2.7 ± 0.2	2.2 ± 0.0	1.5 ± 0.2
Ash (%)	55.4 ± 1.9	72.5 ± 2.6	74.5 ± 0.6	78.9 ± 0.7
Volatiles (%)	36.6 ± 0.7	19.0 ± 0.1	11.4 ± 0.3	6.3 ± 0.3
C fixo (%)	2.0 ± 0.4	6.7 ± 0.7	12.0 ± 0.7	13.2 ± 1.0

Table 1. Proximate analysis of sewage sludge (SS) and sewage sludge biochars (SSB) produced at 350 (SSB₃₅₀), 450 (SSB₄₅₀) and 600 (SSB₆₀₀).

to 900 °C⁵⁴ also yielded a reduction in volatile compounds with increasing temperature. The moisture content of the SS (7.3 ± 0.0%) reduced by approximately five times as much as the SSB₆₀₀ (1.5 ± 0.2%; Table 1). The moisture reduction was attributed to water evaporation and loss of pyrolytic volatiles⁵⁵ relative to SS.

The content of FC, carbon remaining after loss of moisture and free volatile materials of the SSB₆₀₀ (13.2 ± 1.0%) was about seven times higher than that obtained for SS (2.0 ± 0.4%). Working with biochar produced at different pyrolysis temperatures^{5,47} also found similar FC trends. The plot of H/C and FC content (Fig. 3) indicated that the SS material has more H relative to FC, while the biochar produced at high pyrolysis temperatures has less H relative to FC. Working with biochar derived from macaúba endocarp pyrolyzed at temperatures from 200 to 700 °C⁵⁶, reported a similar relationship between H/C and FC. The reduction in the H/C ratio at higher temperatures also results from the breakup of oxygen-containing functional groups, such as carboxyl, carbonyl, and methoxyl, and the formation of aromatic compounds⁵⁷.

Ash accounted for between 72.7% and 81.5% of the proximate analysis components (Table 1). The ash content in the biochar (SSB₃₅₀ 72.5 ± 2.6%, SSB₄₅₀ 74.5 ± 0.6% and SSB₆₀₀ 78.9 ± 0.7%) was higher than in the SS (55.4 ± 1.9%; Table 1). These results are similar to the one reported by Regkouzas and Diamadopoulos⁶⁰, that studying SSB produced at 300 (63.97%), 500 (77.44%) and 700 (81.15%) also found increased ash concentration with pyrolysis temperature and values closed to the ones found in this study. The pyrolysis process impacts not only the biochar ash concentration but also the quality of the material produced, which will be discussed in the following sections.

Physicochemical characteristics. Pyrolysis at different temperatures promoted significant physicochemical changes in the feedstock (Table 2). When compared to feedstock pH (pH_{H₂O} 4.5 and pH_{KCl} 4.2), the biochar acidity was reduced to 1.3 pH_{H₂O} units (pH 4.8 SSB₃₅₀, pH 5.7 SSB₄₅₀, and pH 5.8 SSB₆₅₀) and 1.2 pH_{KCl} units (pH 4.4 SSB₃₅₀, pH 5.3 SSB₄₅₀, and pH 5.4 SSB₆₅₀) with increasing pyrolysis temperature. The increase in biochar pH with thermal treatment has been attributed to the loss of acidic functional groups (carboxyl, hydroxyl, or formyl) on the biochar surface¹. The increase in biochar alkalinity is due to the separation of alkali elements (Ca, Mg, and K) from organic constituents during pyrolysis⁴⁵, which contributes to the potential liming effect. When studying biomass from SS pyrolyzed at 300, 500, and 700 °C⁶⁰, also reported an increase in pH with increasing pyrolysis temperature.

Biochar EC, an estimator of the amount of total dissolved salts in the sample, is one of several biochar properties influenced by the feedstock source and pyrolysis conditions, such as temperature, residence time, and activation treatment^{61,62}. The EC of the SS (4.0 ± 0.0 dS m⁻¹) was higher than that observed for SSB₃₅₀ (2.2 ± 0.0 dS m⁻¹),

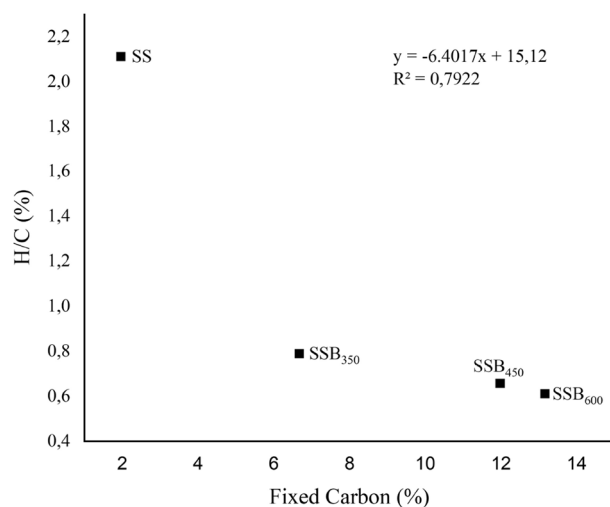


Figure 3. Correlation between ash and fixed carbon of sewage sludge (SS) and sewage sludge biochar (SSB) produced at the pyrolysis temperatures of 350 (SSB₃₅₀), 450 (SSB₄₅₀) and 600 (SSB₆₀₀).

Biochar characteristic	SS	SSB ₃₅₀ ^a	SSB ₄₅₀ ^a	SSB ₆₀₀ ^a
pH _{H2O} (1:10)	4.5 ± 0.1	4.8 ± 0.0	5.7 ± 0.1	5.8 ± 0.0
pH _{KCl} (1:10)	4.2 ± 0.1	4.4 ± 0.0	5.3 ± 0.0	5.4 ± 0.0
EC dSm ⁻¹	4.0 ± 0.0	2.2 ± 0.0	1.6 ± 0.0	1.5 ± 0.3
CEC cmol _c kg ⁻¹	6.0 ± 0.1	6.3 ± 0.1	6.4 ± 0.0	6.0 ± 0.1

Table 2. Physical–chemical characteristics of sewage sludge (SS) and sewage sludge biochars (SSB) produced at 350 (SSB₃₅₀), 450 (SSB₄₅₀) and 600 (SSB₆₀₀).

SSB₄₅₀ (1.6 ± 0.0 dS m⁻¹), and SSB₆₀₀ (1.5 ± 0.0 dS m⁻¹; Table 2). During SS pyrolysis, the ash content increases, whereas the solubility of salts and metals decreases^{63,64}. This occurs because the water-soluble concentrations of K⁺, Ca²⁺, Mg²⁺, and P increase in biochar produced up to 200 °C, but above that temperature it is likely that they will form crystals like whitlockite [(Ca, Mg)₃(PO₄)₂]. At pyrolysis temperatures over 500 °C they will be incorporated into the silicon structure, forming less soluble salts^{58,65}.

The cation exchange capacity (CEC) is one of the most important biochar characteristics because it indicates the potential of the material to attract positively charged ions per unit of mass⁶⁶. In this study, the CEC of the SSB₃₅₀ (6.3 ± 0.1 cmol_c kg⁻¹) and SSB₄₅₀ (6.4 ± 0.0 cmol_c kg⁻¹) were higher than those obtained for both SS and SSB₆₀₀ (6.0 ± 0.1 cmol_c kg⁻¹; Table 2). Biochar produced at temperatures up to 480 °C tends to have higher CEC because some acidic oxygenated functional groups, such as phenolic acid and carboxyl groups, are retained⁶⁷. In contrast, biochar produced at temperatures above 480 °C has lower CEC⁶⁸.

Mineral composition. The total concentrations of some mineral elements are shown in Table 3. The reduction of C, H, S, O, moisture, and volatile content with increasing temperature shows a positive correlation with the increase in concentrations of nonvolatile elements normalized for oxides, such as SiO₂, Al₂O₃, Fe, CaO, and P₂O₅, which are the main mineral components of SS and SSBs. The SiO₂ concentrations in SSB₄₅₀ (43.49 ± 0.11%) and SSB₆₀₀ (40.85 ± 0.11%) were higher than the values observed for SS (33.37 ± 0.09%) and SSB₃₅₀ (33.30 ± 0.29%). In contrast, the increase in Al₂O₃ concentration in the biochar with increasing pyrolysis temperature can be described by linear regression (Al₂O₃% = 0.0097 (Temperature) + 7.3453, R² = 0.86).

The concentration of Al₂O₃ found in this study was lower than the 17.2% and 29.6% reported by Fan et al.⁶⁹ in biochar produced from a cyclic activated sludge system (CSS) process and an applied membrane bioreactor (KSS). The higher Al content was attributed to the presence of inorganic solids from the WWTP. The presence of SiO₂, Al₂O₃, and Fe in biochar is generally associated with the presence of soil material or chemicals used in the coagulation step of SS treatment⁷⁰.

The main macronutrients present in the feedstock were CaO, P₂O₅, and MgO, and Fe, Zn, Mn, and Cu were the main micronutrients. The P₂O₅ concentration (from 2.06 ± 0.01% SS to 2.72 ± 0.05% SSB₆₀₀), and K₂O (from 0.37 ± 0.0% SS to 0.46 ± 0.01% SSB₆₀₀) increased with pyrolysis temperature (Table 3). The effect of pyrolysis on the MgO content was negligible, and there is no clear explanation for CaO reduction (from 2.80 ± 0.00% SS to 2.24 ± 0.01% SSB₄₅₀) with increasing temperature. The MEI of the macronutrients followed the sequence P₂O₅ > K₂O > MgO > CaO (Table 4). The increase in metal enrichment with temperature is due to the

Inorganic components	Sewage sludge	SSB ₃₅₀	SSB ₄₅₀	SSB ₆₀₀	Biochar guidelines
CaO (%)	2.87 ± 0.00	2.61 ± 0.01	2.24 ± 0.01	2.26 ± 0.01	–
P ₂ O ₅ (%)	2.06 ± 0.01	2.49 ± 0.01	2.54 ± 0.03	2.72 ± 0.05	–
MgO (%)	0.96 ± 0.13	1.11 ± 0.16	1.11 ± 0.00	1.04 ± 0.14	–
K ₂ O (%)	0.37 ± 0.0	0.40 ± 0.00	0.47 ± 0.00	0.46 ± 0.01	–
Fe (%)	5.05 ± 0.02	5.78 ± 0.00	5.90 ± 0.00	6.18 ± 0.05	–
Zn (mg kg ⁻¹)	650 ± 30	960 ± 20	1090 ± 20	1120 ± 38	416–7400
Cu (mg kg ⁻¹)	290 ± 0	440 ± 10	510 ± 10	520 ± 10	143–6000
Mn (mg kg ⁻¹)	450 ± 30	510 ± 20	560 ± 30	570 ± 30	–
Pb (mg kg ⁻¹)	50 ± 10	60 ± 10	90 ± 10	80 ± 10	121–300
SiO ₂ (%)	33.37 ± 0.09	33.30 ± 0.26	43.49 ± 0.11	40.85 ± 0.11	–
Al ₂ O ₃ (%)	7.64 ± 0.03	9.38 ± 0.12	12.82 ± 0.06	13.15 ± 0.13	–

Table 3. Mean and standard deviation of the main inorganic components of the biochar as determined by fluorescence X-ray.

Metal	CaO	MgO	K ₂ O	Fe	Zn	Cu	P ₂ O ₅	Mn	Pb	Al ₂ O ₃
SSB ₃₅₀	0.91 ± 0.00	1.16 ± 0.08	1.07 ± 0.01	1.15 ± 0.00	1.48 ± 0.04	1.49 ± 0.04	1.21 ± 0.00	1.12 ± 0.13	1.13 ± 0.15	1.23 ± 0.02
SSB ₄₅₀	0.78 ± 0.00	1.17 ± 0.15	1.27 ± 0.01	1.17 ± 0.01	1.67 ± 0.04	1.76 ± 0.02	1.24 ± 0.02	1.22 ± 0.06	1.65 ± 0.32	1.68 ± 0.01
SSB ₆₀₀	0.79 ± 0.00	1.11 ± 0.23	1.22 ± 0.03	1.22 ± 0.01	1.73 ± 0.07	1.79 ± 0.02	1.32 ± 0.02	1.27 ± 0.16	1.46 ± 0.43	1.72 ± 0.01

Table 4. Metal enrichment Index of the biochar produced at 350 (SSB₃₅₀), 450 (SSB₄₅₀) and 600 (SSB₆₀₀) as compared to the feedstock.

Sample	Cf				Er				PERI
	Cd	Cu	Zn	Pb	Cd	Cu	Zn	Pb	
SS	1.39 ± 0.07	0.03 ± 0.01	1.01 ± 0.10	0.00 ± 0.00	41.65 ± 2.01	0.15 ± 0.01	1.01 ± 0.10	0.00 ± 0.00	42.81 ± 2.08
SSB ₃₅₀	1.22 ± 0.11	0.00 ± 0.00	0.21 ± 0.01	0.00 ± 0.00	36.57 ± 3.17	0.02 ± 0.00	0.21 ± 0.01	0.00 ± 0.00	36.80 ± 3.16
SSB ₄₅₀	3.64 ± 0.53	0.02 ± 0.00	0.12 ± 0.01	0.00 ± 0.00	109.28 ± 15.89	0.10 ± 0.01	0.12 ± 0.01	0.00 ± 0.00	109.50 ± 15.89
SSB ₆₀₀	0.00 ± 0.00	0.02 ± 0.00	0.10 ± 0.01	0.06 ± 0.01	0.00 ± 0.00	0.10 ± 0.00	0.10 ± 0.01	0.29 ± 0.04	0.51 ± 0.04

Table 5. Effect of the pyrolysis temperature on contamination factor (Cf), potential ecological risk coefficient (Er) and potential ecological risk Index (PERI) of the sewage sludge (SS) and sewage sludge biochar produced at 350 (SSB₃₅₀), 450 (SSB₄₅₀) and 600 (SSB₆₀₀).

decomposition of organic matter, which results in the release of the metals associated with organic compounds, and loss of volatile content¹⁸.

Biochar produced from organic residues such as SS has the potential to present high concentrations of PTE, and their content increases with pyrolysis temperature as they form inorganic salts, hydroxides, oxides, and/or sulfides^{18,71}. Similar findings were obtained in this study (Tables 4 and 5), in which the concentration and MEI values of Cu, Zn, Pb, Mn, and Fe increased in line with pyrolysis temperature due to the loss of volatile materials and moisture³, and the high boiling points of PTEs⁷².

The concentration of PTEs in the biochar followed the sequence Fe (from 5.05 ± 0.02% SS to 6.18 ± 0.05% SSB₆₀₀) > Zn (from 650 ± 30 mg kg⁻¹ SS to 1120 ± 38 mg kg⁻¹ SSB₆₀₀) > Mn (450 ± 30 mg kg⁻¹ SS and 570 ± 30 mg kg⁻¹ SSB₆₀₀) > Cu (from 290 ± 0 mg kg⁻¹ SS to 520 ± 10 mg kg⁻¹ SSB₆₀₀; Table 4). The higher Fe concentration in the SS (5.05%) compared to the other PTEs is related to the addition of ferric chloride during sludge aerobic digestion⁷³. The MEI separated the micronutrients into two groups; metals with higher atomic mass (Cu and Zn) were enriched in higher proportions than those of lower atomic mass (Mn and Fe). The PTE concentrations in the SS and biochar used in this study are in agreement with the pollutant control standard of the International Biochar Initiative Guidelines⁷⁴ (Cu from 143 to 6000 mg kg⁻¹ and Zn from 416 to 7400 mg kg⁻¹).

The Pb concentration ranged from 50 mg kg⁻¹ (SS) to 80 mg kg⁻¹ (SSB₆₀₀; Table 3), and the MEI ranged from 1.13 (SSB₃₅₀) to 1.65 (SSB₄₅₀). Based on frequency, toxicity, and potential exposure, Pb is the second most dangerous element behind arsenic (As)⁷⁵. However, the Pb concentration was below the lower limit (121–300 mg kg⁻¹) reported by IBI⁷⁴. Moreover, despite the relevance of the data for content and enrichment of PTE, it must be considered that the estimation of the total metal content is insufficient to assess metal bioavailability, environmental risk, and toxicity, which are controlled by their chemical species rather than their absolute quantities in the samples^{76,77}.

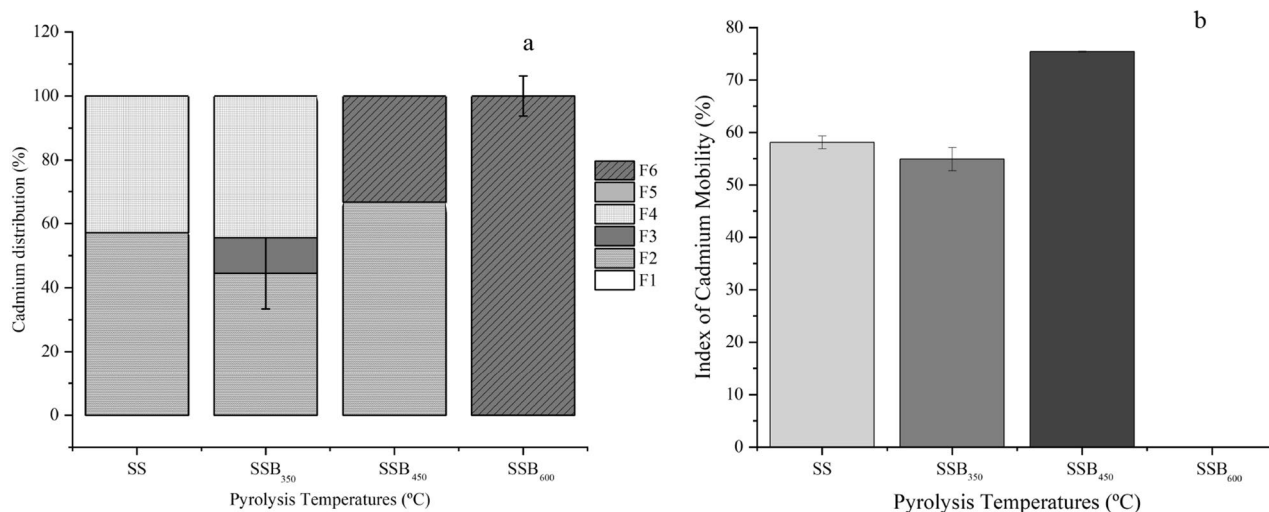


Figure 4. Cadmium fraction distribution (a) and mobility index (b) of sewage sludge biochar produced at 350 (SSB₃₅₀), 450 (SSB₄₅₀) and 600 (SSB₆₀₀).

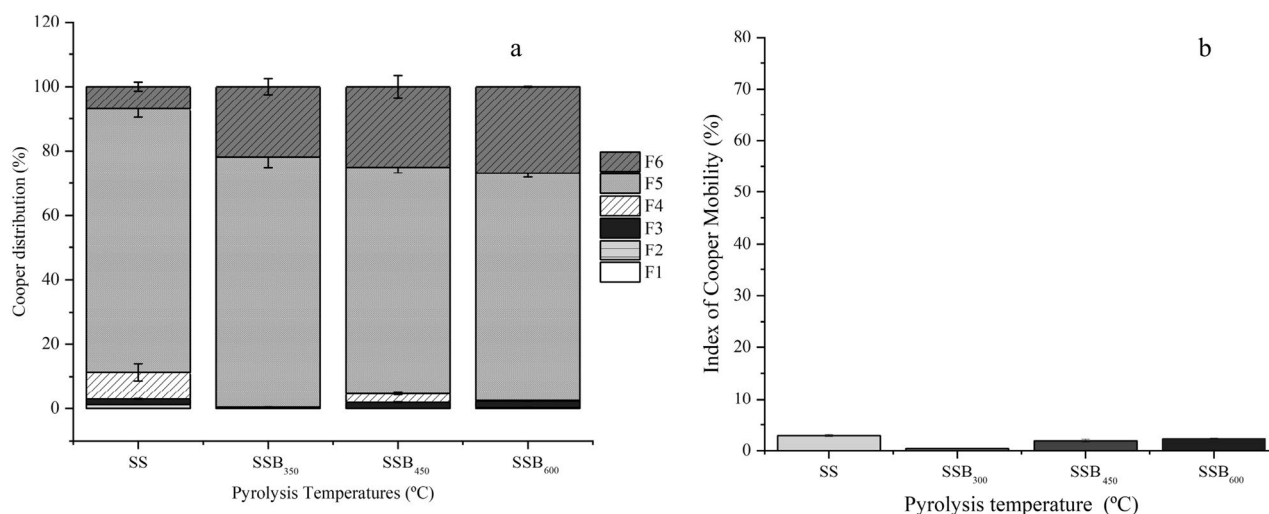


Figure 5. Cooper fraction distribution (a) and mobility index (b) of sewage sludge biochar produced at 350 (SSB₃₅₀), 450 (SSB₄₅₀) and 600 (SSB₆₀₀).

Metal fractionation and metal mobility index. The geochemical forms of PTEs in the environment determine their bioavailability, ecotoxicity, diffusion in mobile forms, and consequently their fate in the environment⁷¹. Metal fractionation is the term used to identify and quantify the different operationally defined species forms or phases in which an element occurs⁷⁸. The fractionation scheme used in this study for quantification of PTEs was based on operationally defined fractions for the following pools: water-soluble (F1), exchangeable (F2), carbonate, (F3), Fe–Mn oxides (F4), organic (F5), and residual (F6) fractions.

The process used in this study for determination of metal availability in the SS and SSBs was adapted from the classifications of Ref.¹⁸. The metals present in the F1, F2, and F3 fractions were classified as bioavailable because they are readily released to the environment. The metals in the F4 and F5 fractions were classified as potentially bioavailable because they are leachable only under very rigorous conditions. The metals in F6 were classified as non-bioavailable because they are unlikely to leach and degrade under natural conditions.

The metal concentrations resulting from USEPA 3050 are given by the sum of all fractions. The extractable fractions of the metals from the SS and SSBs, as well as their mobility index, are shown in Figs. 4, 5, 6 and 7. The total Cd concentration of the SSB₆₀₀ ($1.58 \pm 0.02 \text{ mg kg}^{-1}$) was ~2.5 fold higher than that of the SS ($0.65 \pm 0.02 \text{ mg kg}^{-1}$; Fig. 4a). In contrast to Ref.⁴⁹, where up to 73.3% of the Cd in cow manure biochar produced at 300, 400, 500, 600, and 700 °C was present in the directly toxic and bioavailable fraction, in this study, bioavailable and toxic forms represented $58.11 \pm 1.19\%$ (SS), to $54.86 \pm 2.18\%$ (SS₃₅₀), and $75.41 \pm 6.67\%$ (SSB₄₅₀). All Cd present in SSB₆₀₀ was on the non-bioavailable form (Fig. 4a). Based on the MEI, the Cd present in SSB₆₀₀ poses no risk to humans or microorganisms, whereas SS, SSB₃₅₀, and SSB₄₅₀ have the potential to cause environmental toxicity (Fig. 4b).

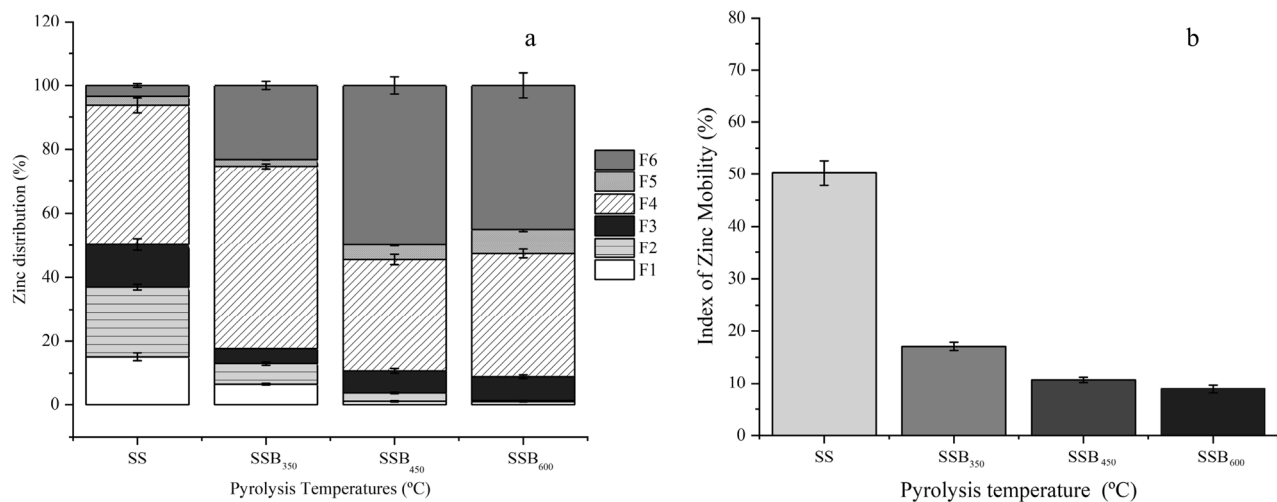


Figure 6. Zinc fraction distribution (a) and mobility index (b) of sewage sludge biochar produced at 350 (SSB₃₅₀), 450 (SSB₄₅₀) and 600 (SSB₆₀₀).

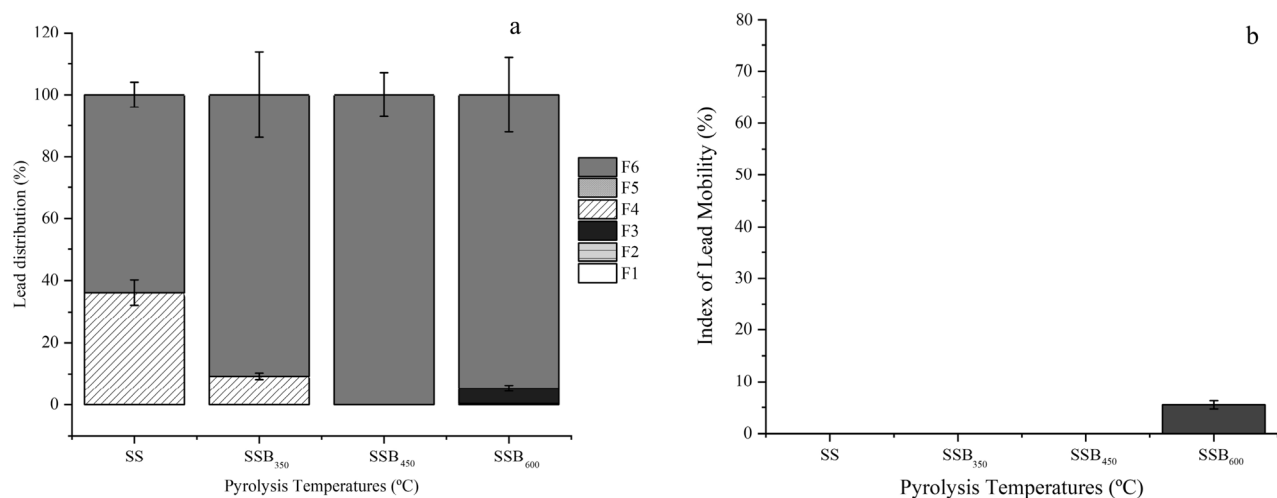


Figure 7. Lead fraction distribution (a) and mobility index (b) of sewage sludge biochar produced at 350 (SSB₃₅₀), 450 (SSB₄₅₀) and 600 (SSB₆₀₀).

The Cu concentration of SSB₆₀₀ ($470.14 \pm 2.14 \text{ mg kg}^{-1}$) was ~ 1.5 -fold greater than that in the SS ($329.53 \pm 4.21 \text{ mg kg}^{-1}$; Fig. 5a). Copper binds readily to organic constituents, forming a highly stable complex⁷⁹. This was observed in this study; in the SS, $2.94 \pm 0.22\%$ of Cu was of the toxic bioavailable form, and $90.15 \pm 1.37\%$ was of the potentially bioavailable form (Fig. 5a). As the pyrolysis temperature increased, most of the Cu was distributed in potentially bioavailable (SSB₃₅₀ $77.77 \pm 2.12\%$, SSB₄₅₀ $73.07 \pm 2.47\%$, and SSB₆₀₀ $70.69 \pm 0.29\%$) and non-bioavailable (SSB₃₅₀ $21.81 \pm 2.19\%$, SSB₄₅₀ $24.96 \pm 2.64\%$, and SSB₆₀₀ $27.01 \pm 0.34\%$) forms. These results are similar to those reported by Lu et al.⁸⁰ where study of SSBs produced at 300, 400, 500, 600, and 700 °C showed that most of the Cu was concentrated in the potentially available and non-available fractions. In this study, 96.3–100% of the potentially available Cu was in the organic fraction. The Cu enrichment in the biochar increased in line with the pyrolysis temperature (SSB₃₅₀ 0.42%, SSB₄₅₀ 1.92%, and SSB₆₀₀ 2.31%); however, since most of the metal is of potentially bioavailable and non-bioavailable forms, this enrichment is not associated with its increase in ecotoxicity (Fig. 5b). Moreover, the Cu MEI in the SSBs was lower than that observed in the SS.

Zinc content in the SSB₆₀₀ ($665.82 \text{ mg kg}^{-1}$) was 1.4 times higher than the SS ($487.40 \text{ mg kg}^{-1}$), and its distribution in the biochar fraction was greatly influenced by the pyrolysis temperature (Fig. 6a). The bioavailable Zn reduced with increasing temperature, which facilitated the transformation of the metal to the potentially bioavailable (SS 46.32 ± 2.51 , SSB₃₅₀ 59.25 ± 0.24 , SSB₄₅₀ 39.48 ± 0.26 , and SSB₆₀₀ $46.10 \pm 1.76\%$) and residual (SS 3.43 ± 0.57 , SSB₃₅₀ 23.15 ± 0.89 , SSB₄₅₀ 49.84 ± 0.49 , and SSB₆₀₀ $45.02 \pm 2.52\%$) forms. Between 83.5 and 96.3% of the potentially bioavailable Zn was in the reduced oxide fraction. The Zn MEI was $17.60 \pm 0.83\%$ for SSB₃₅₀, $10.68 \pm 0.54\%$ for SSB₄₅₀ and 8.88 ± 0.00 for SSB₆₀₀ (Fig. 6b). According to Li et al.⁸¹, the low mobility of Cr, Ni, Cu, Zn, Cd, Pb, and Hg in sewage sludge biochar is due to their alkaline properties.

Cf	Er	PERI	Ecological risk
< 1	≤ 40	PERI ≤ 150	Low contamination
1 < Cf ≤ 3	40 < Er ≤ 80	150 < Er ≤ 300	Moderate contamination
3 < Cf ≤ 6	80 < Er ≤ 160	300 < Er ≤ 600	Considerable contamination
6 < Cf ≤ 9	160 < Er ≤ 320	PERI > 600	High risk
Cf > 9	Er ≥ 320	–	Very high contamination

Table 6. Grading of contamination factor (Cf), the potential ecological risk coefficient (Er) and potential ecological risk index (PERI).

Lead content varied from $19.94 \pm 1.52 \text{ mg kg}^{-1}$ (SS) to $31.69 \pm 3.83 \text{ mg kg}^{-1}$ (SSB₆₀₀). At least 91% of the Pb present in the SSBs was non-bioavailable (Fig. 7a). Similar to this study, evaluation by Wang et al.⁵⁹ of biochar produced at temperatures of 300, 500, and 700 °C from hydrothermal pretreatment with pyrolysis (HTP) suggested that up to 99.97% of the Pb was in the residual fraction. Although Pb had the lowest MMI of all the metals studied, the index increased in line with temperature (SS 0.00 ± 0.00 , SSB₃₅₀ 0.00 ± 0.00 , SSB₄₅₀ 0.00 ± 0.00 and SSB₆₀₀ 5.50 ± 0.78 ; Fig. 7b). The predominance of Pb in the residual fraction may be associated with the combination of the metal with primary minerals in the SS⁵⁹.

Risk analysis of potentially toxic elements. The risk to the environment and organisms posed by PTEs present in the SS and SSBs produced at different pyrolysis temperature was assessed by calculating the PERI (Table 5). Among the PTEs, Cd and Zn were the only metals that presented Cf values in the range of contamination. Cadmium Cf values increased in line with pyrolysis temperature, and the risk of contamination ranked from moderate for SS (1.39 ± 0.07) and SSB₃₅₀ (1.22 ± 0.11), to considerable for SSB₄₅₀ (3.64 ± 0.53), while Zn Cf values reduced in line with pyrolysis temperature, and only SS (1.01 ± 0.10) had a Cf value in the range for moderate contamination (Tables 5 and 6). The Pb and Cu Cfs were below the contamination values. According to Ref.¹⁸, the Cf of individual PTEs measures the degree of pollution by individual heavy metals, and its value is inversely proportional to its leaching potential.

The index of potential ecological risk individuals, given by Er, is a function of the biological toxicity factor of individual PTEs²⁷. Cadmium, present in the SS (41.65 ± 2.01) and SSB₄₅₀ (109.28 ± 15.89), was the only metal with the individual potential ecological risk index value in the moderate (SS 41.65 ± 2.01) to considerable (SSB₄₅₀ 109.28 ± 15.89) contamination range. The pyrolysis temperature had a significant effect on reduction of the Er values for the other metals studied (Table 5).

The potential ecological risk index (PERI) measured the degree of superposition of various harmful PTEs on organisms and the environment⁸¹. As reported in other studies^{59,82}, the increase in pyrolysis temperature had a positive benefit on reducing the PERI value (SSB₃₅₀ $36.80 \pm 3.16\%$, and SSB₆₀₀ $0.51 \pm 0.04\%$) as compared with SS ($42.81 \pm 2.08\%$). The SSB₄₅₀ ($109.50\% \pm 15.89$) presented a PERI value of 155.76%, higher than that for SS, because of the increase in Cd availability. Despite the SSB₄₅₀ PERI value, the four PTEs have values that suggest a low potential ecological risk for utilization of biochar.

Conclusions

The effects of pyrolysis temperature on sewage sludge biochar physicochemical properties were evaluated. The pyrolysis temperature affects the ultimate and proximate composition, the stability, aromaticity, and polarity of the biochar produced at different temperature. Moreover, the pyrolysis temperature also influenced the concentration of inorganic macro (Ca, Mg, P₂O₅, and K₂O), micronutrients (Cu and Zn), and some toxic elements such as Pb and Cd. The pyrolysis temperature also has an important contribution in the transformation of metals from more toxic and available forms into more stable nontoxic and non-available forms. Based on the individual potential ecological risk index, Cd in the SS and SSB₄₅₀ was in the moderate and considerable contamination ranges, respectively, and was the metal with the highest contribution to the PERI. Despite this contribution, the potential ecological risk index of the SS and SSBs was graded as low-risk.

Received: 9 April 2020; Accepted: 25 September 2020

Published online: 13 January 2021

References

- Weber, K. & Quicker, P. Properties of biochar. *Fuel* **217**, 240–261 (2018).
- Jeffery, S., Verheijen, F. G. A., Van Der Velde, M. & Bastos, A. C. A quantitative review of the effects of biochar application to soils on crop productivity using meta-analysis. *Agric. Ecosyst. Environ.* **144**, 175–187 (2011).
- Chan, K. Y. & Xu, Z. Biochar para o meio ambiente ciência e tecnologia de gestão. In *Biochar: Propriedades dos nutrientes e seus Aprimoramento* (eds. Lehmann, J. & Joseph, S.) 67–84 (Earthscan, Londres, 2009).
- Frišták, V. & Soja, G. Effect of wood-based biochar and sewage sludge amendments for soil phosphorus availability. *Nov. Biotechnol. Chim.* <https://doi.org/10.1515/nbec-2015-0020> (2015).
- Hossain, M. K., Strezov, V., Chan, K. Y., Ziolkowski, A. & Nelson, P. F. Influence of pyrolysis temperature on production and nutrient properties of wastewater sludge biochar. *J. Environ. Manag.* **92**, 223–228 (2011).
- Liu, C., Yang, J., Wang, G. & Ye, B. Impact of application of biochar-based fertilizer on the content of phosphorus and potassium in soil. In *IOP Conference Series: Earth and Environmental Science*. vol. 252 (2019).

7. Jin, J. *et al.* Cumulative effects of bamboo sawdust addition on pyrolysis of sewage sludge: biochar properties and environmental risk from metals. *Bioresour. Technol.* **228**, 218–226 (2016).
8. Lehmann, J., Gaunt, J. & Rondon, M. Bio-char sequestration in terrestrial ecosystems—a review. *Mitig. Adapt. Strateg. Glob. Change* **11**, 403–427 (2006).
9. Ahmad, M. *et al.* Biochar as a sorbent for contaminant management in soil and water: a review. *Chemosphere* **99**, 19–23 (2014).
10. Xie, T., Reddy, K. R., Wang, C., Yargicoglu, E. & Spokas, K. Characteristics and applications of biochar for environmental remediation: a review. *Crit. Rev. Environ. Sci. Technol.* **45**, 939–969 (2015).
11. Ndirangu, S. M., Liu, Y., Xu, K. & Song, S. Risk evaluation of pyrolyzed biochar from multiple wastes. *J. Chem.* **2019**, 1–28 (2019).
12. Agrafioti, E., Bouras, G., Kalderis, D. & Diamadopoulos, E. Biochar production by sewage sludge pyrolysis. *J. Anal. Appl. Pyrolysis* **101**, 72–78 (2013).
13. Zielińska, A. & Oleszczuk, P. The conversion of sewage sludge into biochar reduces polycyclic aromatic hydrocarbon content and ecotoxicity but increases trace metal content. *Biomass Bioenergy* **75**, 235–244 (2015).
14. Paz-Ferreiro, J., Nieto, A., Méndez, A., Askeland, M. P. J. & Gascó, G. Biochar from Biosolids Pyrolysis: A Review. *Int. J. Environ. Res. Public Health* **15**, 1–16 (2018).
15. Chen, T. *et al.* Adsorption of cadmium by biochar derived from municipal sewage sludge: impact factors and adsorption mechanism. *Chemosphere* **134**, 286–293 (2015).
16. Qiang, L., Wen-Zhi, L. & Xi-Feng, Z. Overview of fuel properties of biomass fast pyrolysis oils. *Energy Convers. Manag.* **50**, 1376–1383 (2009).
17. Spokas, K. Review of the stability of biochar in soils: predictability of O:C molar ratios. *Carbon Manag.* **1**, 289–303 (2010).
18. Devi, P. & Saroha, A. K. Risk analysis of pyrolyzed biochar made from paper mill effluent treatment plant sludge for bioavailability and eco-toxicity of heavy metals. *Bioresour. Technol.* **162**, 308–315 (2014).
19. Camps Arbustain, M., Saggarr, S. & Leifeld, J. Environmental benefits and risks of biochar application to soil. *Agric. Ecosyst. Environ.* **191**, 1–4 (2014).
20. Schimmelpfennig, S. & Glaser, B. One step forward toward characterization: some important material properties to distinguish biochars. *J. Environ. Qual.* **41**, 1001–1013 (2012).
21. Kim, H. S. *et al.* Effect of biochar on heavy metal immobilization and uptake by lettuce (*Lactuca sativa* L.) in agricultural soil. *Environ. Earth Sci.* **74**, 1249–1259 (2015).
22. Brinton Junior, W. F. Characterization of man-made foreign matter and its presence in multiple size fractions from mixed waste composting. *Compos. Sci. Util.* **13**, 274–280 (2005).
23. Cowie, A. L. *et al.* Is sustainability certification for biochar the answer to environmental risks?. *Pesqui. Agropecu. Bras.* **47**, 637–648 (2012).
24. Sigmund, G. *et al.* Cytotoxicity of biochar: a workplace safety concern?. *Environ. Sci. Technol. Lett.* **4**, 362–366 (2017).
25. Su, D. C. & Wong, J. W. C. Chemical speciation and phytoavailability of Zn, Cu, Ni and Cd in soil amended with fly ash-stabilized sewage sludge. *Environ. Int.* **29**, 895–900 (2003).
26. Flyhammar, P. Use of sequential extraction on anaerobically degraded municipal solid waste. *Sci. Total Environ.* **212**, 203–215 (1998).
27. Hakanson, L. An ecological risk index for aquatic pollution control—a sedimentological approach. *Water Res.* **14**, 975–1001 (1980).
28. Schwarzenbach, R. P. *et al.* The challenge of micropollutants in aquatic systems. *Science (80-)* **313**, 1072–1077 (2006).
29. Enders, A. & Lehmann, J. Proximate analyses for characterising biochars. In *Biochar: A Guide to Analytical Methods* (eds Singh, B. *et al.*) 310 (CRC Press, Boca Raton, 2017).
30. USEPA. Fiel portable X-Ray fluorescence spectrometry for the determination of elemental concentrations in soil and sediment. *United States Environ. Prot. Agency* **67**, 14–21 (2007).
31. USEPA. Method 3050B. Acid digestion of sediments, sludges, and soils. *United States Environ. Prot. Agency* **18**, 723 (1996).
32. Aston, S. *et al.* The impacts of pyrolysis temperature and feedstock type on biochar properties and the effects of biochar application on the properties of a sandy loam. *Geophys. Res. Abstr.* **15**, EGU2013-11083 (2013).
33. Tan, L. L., Ahmad, M. & Lee, Y. H. A novel optical ammonia sensor based on reflectance measurements for highly polluted and coloured water. *Sens. Actuators B Chem.* **171–172**, 994–1000 (2012).
34. Tessier, A., Campbell, P. G. C. & Bisson, M. Sequential extraction procedure for the speciation of particulate trace metals. *Anal. Chem.* **51**, 844–851 (1979).
35. Kabala, C. & Singh, B. R. Fractionation and mobility of copper, lead, and zinc in soil profiles in the vicinity of a copper smelter. *J. Environ. Qual.* **30**, 485–492 (2001).
36. Douay, F. *et al.* Assessment of potential health risk for inhabitants living near a former lead smelter. Part 1: metal concentrations in soils, agricultural crops, and homegrown vegetables. *Environ. Monit. Assess.* **185**, 3665–3680 (2013).
37. SPSS. *SPSS Statistics V25* (2017).
38. Tripathi, M., Sahu, J. N. & Ganesan, P. Effect of process parameters on production of biochar from biomass waste through pyrolysis: A review. *Renew. Sustain. Energy Rev.* **55**, 467–481 (2016).
39. Qambrani, N. A., Rahman, M. M., Won, S., Shim, S. & Ra, C. Biochar properties and eco-friendly applications for climate change mitigation, waste management, and wastewater treatment: a review. *Renew. Sustain. Energy Rev.* **79**, 255–273 (2017).
40. Lu, T. *et al.* On the pyrolysis of sewage sludge: the influence of pyrolysis temperature on biochar, liquid and gas fractions. *Adv. Mater. Res.* **518–523**, 3412–3420 (2012).
41. Antal, M. J. & Gronli, M. The art, science, and technology of charcoal production. *Ind. Eng. Chem. Res.* **42**, 1619–1640 (2003).
42. Quicker, P. & Weber, K. *Biokohle: Herstellung, Eigenschaften und Verwendung von Biomassekarbonisaten* (Springer, Berlin, 2016).
43. Bagreev, A., Badosz, T. J. & Locke, D. C. Pore structure and surface chemistry of adsorbents obtained by pyrolysis of sewage sludge-derived fertilizer. *Carbon N. Y.* **39**, 1971–1979 (2001).
44. Cantrell, K. B., Hunt, P. G., Uchimiya, M., Novak, J. M. & Ro, K. S. Impact of pyrolysis temperature and manure source on physicochemical characteristics of biochar. *Bioresour. Technol.* **107**, 419–428 (2012).
45. Al-Wabel, M. I., Al-Omran, A., El-Naggar, A. H., Nadeem, M. & Usman, A. R. A. Pyrolysis temperature induced changes in characteristics and chemical composition of biochar produced from conocarpus wastes. *Bioresour. Technol.* **131**, 374–379 (2013).
46. Ro, K. S., Cantrell, K. B. & Hunt, P. G. High-temperature pyrolysis of blended animal manures for producing renewable energy and value-added biochar. *Ind. Eng. Chem. Res.* **49**, 10125–10131 (2010).
47. Uchimiya, M., Chang, S. C. & Klasson, K. T. Screening biochars for heavy metal retention in soil: role of oxygen functional groups. *J. Hazard. Mater.* **190**, 432–441 (2011).
48. Qayyum, M. F., Steffens, D., Reisenauer, H. P. & Schubert, S. Biochars influence differential distribution and chemical composition of soil organic matter. *Plant Soil Environ.* **60**, 337–343 (2014).
49. Zhang, P., Zhang, X., Li, Y. & Han, L. Influence of pyrolysis temperature on chemical speciation, leaching ability, and environmental risk of heavy metals in biochar derived from cow manure. *Bioresour. Technol.* <https://doi.org/10.1016/j.biortech.2020.122850> (2020).
50. Chen, T. *et al.* Influence of pyrolysis temperature on characteristics and heavy metal adsorptive performance of biochar derived from municipal sewage sludge. *Bioresour. Technol.* **164**, 47–54 (2014).
51. Yuan, J. H., Xu, R. K. & Zhang, H. The forms of alkalis in the biochar produced from crop residues at different temperatures. *Bioresour. Technol.* **102**, 3488–3497 (2011).

52. Jindo, K., Mizumoto, H., Sawada, Y. & Sonoki, T. Physical and chemical characterization of biochars derived from. *Biogeosciences* **11**, 6613–6621 (2014).
53. Hu, Y. *et al.* Thermal transformation of carbon and oxygen-containing organic compounds in sewage sludge during pyrolysis treatment. *Energies* **12**, 1–13 (2019).
54. Zhang, J. *et al.* Multiscale visualization of the structural and characteristic changes of sewage sludge biochar oriented towards potential agronomic and environmental implication. *Sci. Rep.* **5**, 1–8 (2015).
55. Neves, D., Thunman, H., Matos, A., Tarelho, L. & Gómez-barea, A. Characterization and prediction of biomass pyrolysis products. *Prog. Energy Combust. Sci.* **37**, 611–630 (2011).
56. Guilhen, S. N., Mašek, O., Ortiz, N., Izidoro, J. C. & Fungaro, D. A. Pyrolytic temperature evaluation of macauba biochar for uranium adsorption from aqueous solutions. *Biomass Bioenergy* **122**, 381–390 (2019).
57. Ma, Z. *et al.* Evolution of the chemical composition, functional group, pore structure and crystallographic structure of bio-char from palm kernel shell pyrolysis under different temperatures. *J. Anal. Appl. Pyrolysis* <https://doi.org/10.1016/j.jaap.2017.07.015> (2017).
58. Cao, X., Ma, L., Liang, Y., Gao, B. & Harris, W. Simultaneous immobilization of lead and atrazine in contaminated soils using dairy-manure biochar. *Environ. Sci. Technol.* **45**, 4884–4889 (2011).
59. Wang, X., Chi, Q., Liu, X. & Wang, Y. Influence of pyrolysis temperature on characteristics and environmental risk of heavy metals in pyrolyzed biochar made from hydrothermally treated sewage sludge. *Chemosphere* <https://doi.org/10.1016/j.chemosphere.2018.10.189> (2019).
60. Regkhouzas, P. & Diamadopoulos, E. Adsorption of selected organic micro-pollutants on sewage sludge biochar. *Chemosphere* **224**, 840–851 (2019).
61. Bird, M. I., Wurster, C. M., de Paula Silva, P. H., Bass, A. M. & de Nys, R. Algal biochar—production and properties. *Bioresour. Technol.* **102**, 1886–1891 (2011).
62. Lu, H. *et al.* Characterization of sewage sludge-derived biochars from different feedstocks and pyrolysis temperatures. *J. Anal. Appl. Pyrolysis* **102**, 137–143 (2013).
63. de Figueredo, N. A., da Costa, L. M., Melo, L. C. A., Siebeneichler, E. A. & Tronto, J. Characterization of biochars from different sources and evaluation of release of nutrients and contaminants. *Rev. Cienc. Agron.* **48**, 395–403 (2017).
64. Tian, Y., Cui, L., Lin, Q., Li, G. & Zhao, X. The sewage sludge biochar at low pyrolysis temperature had better improvement in urban soil and turf grass. *Agronomy* **9**, 156. <https://doi.org/10.3390/agronomy9030156> (2019).
65. Shinogi, Y. Nutrient leaching from carbon. In *ASAE/CSAE Annual International Meeting Meeting*. (2004).
66. Bibar, M. P. S. *Potencial Agrícola de Biocarvões Provenientes de Biomassas Alternativas* (Instituto Agronômico de Campinas, Campinas, 2014). <https://doi.org/10.1017/CBO9781107415324.004>.
67. Mitchell, P. J., Dalley, T. S. L. & Helleur, R. J. Preliminary laboratory production and characterization of biochars from lignocellulosic municipal waste. *J. Anal. Appl. Pyrolysis* **99**, 71–78 (2013).
68. Novak, J. M. *et al.* Impact of biochar amendment on fertility of a southeastern coastal plain soil. *Soil Sci.* **174**, 105–112 (2009).
69. Fan, J. *et al.* Using sewage sludge with high ash content for biochar production and Cu (II) sorption. *Sci. Total Environ.* **713**, 136663 (2020).
70. Oh, T. K., Choi, B., Shinogi, Y. & Chikushi, J. Effect of pH conditions on actual and apparent fluoride adsorption by biochar in aqueous phase. *Water. Air. Soil Pollut.* **223**, 3729–3738 (2012).
71. Callegari, A., Hlavinek, P. & Capodaglio, A. G. Production of energy (biodiesel) and recovery of materials (biochar) from pyrolysis of urban waste sludge. *Rev. Ambient. Água* **13**(2), 2128. <https://doi.org/10.4136/ambi-agua.2128> (2018).
72. Wesenbeeck, S. V., Prins, W., Ronsse, F. & Antal, M. J. sewage sludge carbonization for biochar applications. *Fate Heavy Met.* <https://doi.org/10.1021/ef500875c> (2014).
73. Barry, D., Barbiero, C., Briens, C. & Berruti, F. Pyrolysis as an economical and ecological treatment option for municipal sewage sludge. *Biomass Bioenergy* **122**, 472–480 (2019).
74. International Biochar Initiative. Standardized product definition and product testing guidelines for biochar that is used in soil. *Int. Biochar Initiat.* **23** (2015).
75. ATSDR. Substance Priority List | ATSDR. *Agency for Toxic Substances and Disease Registry* (2019). Available at: <https://www.atsdr.cdc.gov/spl/index.html#2019spl>. Accessed 7 April 2020.
76. Yuan, X. *et al.* Bioresource technology total concentrations and chemical speciation of heavy metals in liquefaction residues of sewage sludge. *Bioresour. Technol.* **102**, 4104–4110 (2011).
77. Huang, H. & Yuan, X. Bioresource technology the migration and transformation behaviors of heavy metals during the hydrothermal treatment of sewage sludge. *Bioresour. Technol.* **200**, 991–998 (2016).
78. Bogusz, A. & Oleszczuk, P. Sequential extraction of nickel and zinc in sewage sludge-or biochar/sewage sludge-amended soil. *Sci. Total Environ.* **636**, 927–935 (2018).
79. Shi, W. *et al.* Bioresource technology immobilization of heavy metals in sewage sludge by using subcritical water technology. *Bioresour. Technol.* **137**, 18–24 (2013).
80. Lu, Y. *et al.* Impacts of soil and water pollution on food safety and health risks in China. *Environ. Int.* **77**, 5–15 (2015).
81. Li, F. *et al.* Spatial risk assessment and sources identification of heavy metals in surface sediments from the Dongting Lake, Middle China. *J. Geochem. Explor.* **132**, 75–83 (2013).
82. Leng, L. *et al.* Bioresource technology the migration and transformation behavior of heavy metals during the liquefaction process of sewage sludge. *Bioresour. Technol.* **167**, 144–150 (2014).

Acknowledgments

We would like to thank the graduate program of Soil and Quality of the Ecosystem of the University Federal of the Recôncavo of Bahia; Bahia Research Foundation of Support (FAPESB) App. 0093/2016 for the financial support, and Coordination for the Improvement of Higher Education Personnel (CAPES) for the scholarship, the Bahian Water and Sanitation Company (EMBASA) for providing the sewage sludge, and the Company BahiaCarbon Agro-industry LTDA for so kindly have pyrolyzed the sewage sludge.

Author contributions

The manuscript is part of the dissertation of the first author C.S.S., which had the support from L.S.A., W.N.S., M.C.A. for laboratory analyzes. J.A.G.S. and M.R.B., adviser and co-adviser, respectively, translated the document.

Competing interests

The authors declare no competing interests.

Additional information

Correspondence and requests for materials should be addressed to M.R.B.

Reprints and permissions information is available at www.nature.com/reprints.

Publisher's note Springer Nature remains neutral with regard to jurisdictional claims in published maps and institutional affiliations.



Open Access This article is licensed under a Creative Commons Attribution 4.0 International License, which permits use, sharing, adaptation, distribution and reproduction in any medium or format, as long as you give appropriate credit to the original author(s) and the source, provide a link to the Creative Commons licence, and indicate if changes were made. The images or other third party material in this article are included in the article's Creative Commons licence, unless indicated otherwise in a credit line to the material. If material is not included in the article's Creative Commons licence and your intended use is not permitted by statutory regulation or exceeds the permitted use, you will need to obtain permission directly from the copyright holder. To view a copy of this licence, visit <http://creativecommons.org/licenses/by/4.0/>.

© The Author(s) 2021